Available online at www.sciencedirect.com

ScienceDirect

Physics Procedia 67 (2015) 60 – 65

Physics Procedia

25th International Cryogenic Engineering Conference and the International Cryogenic Materials Conference in 2014, ICEC 25–ICMC 2014

Conceptual design of the cryogenic system for the high-luminosity upgrade of the Large Hadron Collider (LHC)

K. Brodzinski, S. Claudet, G. Ferlin, L. Tavian *, U. Wagner, R. Van Weelderen

Technology Department, CERN, 1211 Geneva 23, Switzerland

Abstract

The discovery of a Higgs boson at CERN in 2012 is the start of a major program of work to measure this particle's properties with the highest possible precision for testing the validity of the Standard Model and to search for further new physics at the energy frontier. The LHC is in a unique position to pursue this program. Europe's top priority is the exploitation of the full potential of the LHC, including the high-luminosity upgrade of the machine and detectors with an objective to collect ten times more data than in the initial design, by around 2030. To reach this objective, the LHC cryogenic system must be upgraded to withstand higher beam current and higher luminosity at top energy while keeping the same operation availability by improving the collimation system and the protection of electronics sensitive to radiation. This paper will present the conceptual design of the cryogenic system upgrade with recent updates in performance requirements, the corresponding layout and architecture of the system as well as the main technical challenges which have to be met in the coming years.

Peer-review under responsibility of the organizing committee of ICEC 25-ICMC 2014

Keywords: particle accelerator; superconducting magnet; RF cavity; helium cryogenics; superfluid helium; Large Hadron Collider

1. Introduction

The upgrade of the LHC [Rossi et al. (2012)] aiming to collect ten times more data than in the initial design will require increasing the bunch population from 115 to 220 billion of protons per bunch and the luminosity in the

* Corresponding author. Tel.: +41 22 767 6959;
E-mail address: Laurent.tavian@cern.ch

Peer-review under responsibility of the organizing committee of ICEC 25-ICMC 2014
doi:10.1016/j.phpro.2015.06.011

ATLAS and CMS detector by a factor of 5. Consequently, higher beam-induced heating will impact the cryogenic system, which will require a major upgrade. This upgrade will consist of the design and installation of two new cryogenic plants at point 1 and point 5 for the high luminosity insertions dedicated to the large ATLAS and CMS detectors, the design and installation of a new cryogenic plant at point 4 for superconducting radio-frequency (SRF) modules, the design of new cryogenic circuits at point 1, point 5 and point 7 for high-temperature superconducting (HTS) links and displaced current feed boxes, as well as cryogenic design for cryo-collimators and 11 T dipoles.

2. Main LHC machine upgrade

2.1. New collimation scheme

The collimation scheme must be upgraded by adding collimators in particular in the continuous cryostat close to points 2 and 7, and may be also at points 3, 1 and 5. The corresponding integration space must be created by developing shorter but stronger 11 T superconducting dipole magnets. As the new collimators will work at room temperature, cryogenic bypasses are required to guarantee the continuity of the cryogenic and electrical distribution. Fig. 1 shows the nominal and upgraded layouts of the continuous cryostat.

Halo control may require also the installation of hollow electron lenses at point 4 (see Fig. 3), making use of a superconducting solenoid. While not yet in the baseline, this device may be the best option for controlling particle diffusion speed.

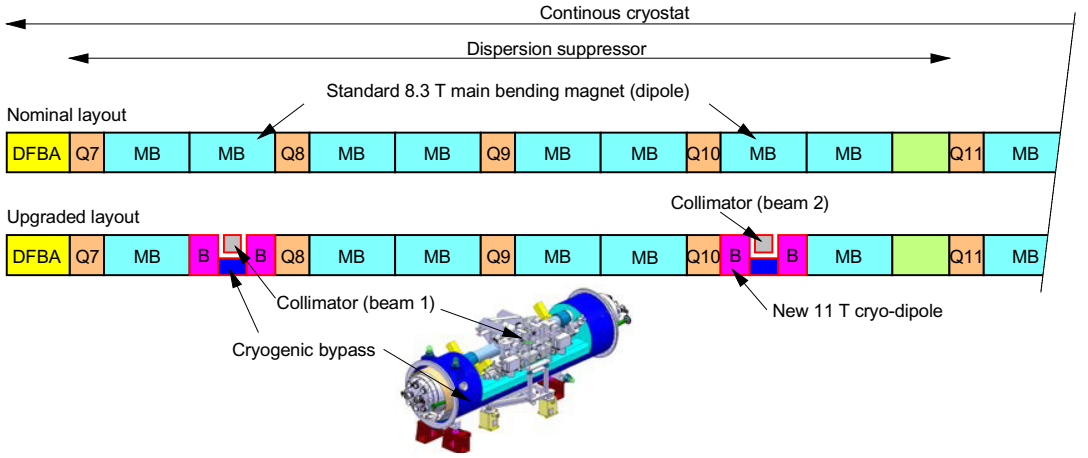

Fig. 1. Nominal and upgraded layouts of the continuous cryostat.

2.2. New cold-powering scheme

The increase of the level of radiation to electronics in the tunnel will require relocating power convertors and related current feed boxes in an access gallery at point 7 and at ground level at points 1 and 5. New superconducting links based on high-temperature superconducting (HTS) technology will be required to connect the displaced current feed boxes to the magnets and will carry total currents from 80 kA to 220 kA. Fig. 2 and Fig. 4 show the nominal and upgraded layouts of the insertion regions respectively at point 7 and at points 1 & 5.

2.3. New SRF system at Point 4

To better control the bunch longitudinal profile, to reduce heating and to improve the pile-up density, two (one per beam) new SRF modules equipped with 800-MHz cavities will be added to the existing 400 MHz SRF modules at point 4 creating a high-harmonic radio-frequency system (see Fig. 3).

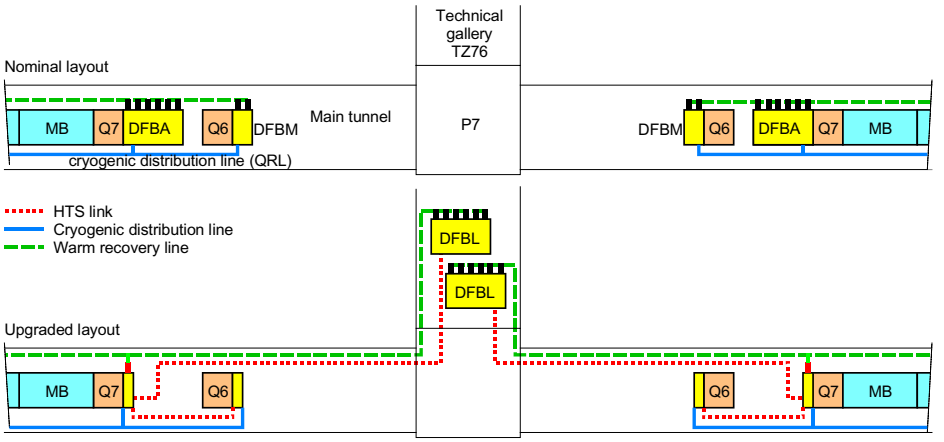

Fig. 2. Nominal and upgraded layouts of powering at Point 7.

2.4. New insertions at points 1 and 5

The matching section and final focusing of the beams will require completely new insertions cryo-magnets [Todesco et al. (2013)] at points 1 and 5 (see Fig. 4). In addition, to improve the luminosity performance, by recovering the geometric luminosity reduction factor and to allow the levelling of the luminosity to limit the total number of collisions per bunch at the maximum acceptable value for the high-luminosity detectors, two cryo-modules of six (three per beam) crab-cavities (CC) will be added at points 1 and at point 5 [Calaga (2012)].

3. Temperature levels and heat loads

For new equipment, the specific thermal performance of supporting systems, radiative insulation and thermal shields is identical to the one of existing LHC equipment.

The upgraded proton-bunch population will increase the beam-induced heating composed of synchrotron radiation, beam image current and electron-clouds impingement. This heating will impact the whole accelerator and is mainly deposited on the beam-screens. The main concern remains the electron-cloud impingement which can only be reduced by an efficient beam scrubbing of the beam screens which is today not demonstrated. Without efficient scrubbing, the e-cloud activity will remain high (more than 4 W per meter and per beam) in the arcs and dispersion suppressors. This heat deposition corresponds to about twice the local cooling limitation given by the hydraulic impedance of the beam screen cooling circuits.

The upgraded luminosity at point 1 and 5 will increase the deposition of secondary particles escaping from the detectors. This deposition of about 1280 W per half insertion will mainly impact the final focusing quadrupoles (Q1 to Q3). The beam screens of these new quadrupoles [Todesco et al. (2012)] will be equipped with tungsten shielding which will be able to stop about half of the total secondary particle deposition. This shielding reduces the overall refrigeration cost and increases the life time of the inner-triplet coils. The heat deposition in the superconducting coil inside the magnet cold-masses of the inner triplets reaches 5 W/cm^3 creating temperature difference in the superconducting cables with respect to the main bath operating at 1.9 K [Granieri et al. (2013)]. Sufficient margin with respect to resistive transition limit must be guaranteed [Granieri et al. (2013)].

Table 1 gives the operating conditions of the different new equipment and their cooling methods. Like for the sector, the thermal shields are cooled between 50 and 75 K. As concerns the beam screens, the baseline is a cooling with supercritical helium at 3 bar between 4.6 and 20 K. As the load on the beam screens of the new inner triplets is very high, an alternative cooling with supercritical helium at 20 bar between 40 and 60 K, a temperature range compatible with vacuum and longitudinal-impedance requirements, is under study to reduce the corresponding refrigeration cost and the diameter of the cooling capillaries of the beam screens (Baglin et al. (2012)).

Table 1. Operating conditions and cooling methods.

Equipment	Operating condition [K]	Operating condition [bar]	Cooling method
11-T cryo-dipole (P1, P2, P5 & P7)	1.9	1.3	In static pressurized superfluid helium via a bayonet heat exchanger Φ 54 mm
Cryogenic bypass (P1, P2, P5 & P7)	1.9	1.3	In static pressurized superfluid helium and conduction cooled by adjacent 11-T cryo-dipoles
RF cryo-module 800 MHz (P4)	4.5	1.3	Pool boiling in saturated helium
Electron lens (P4)	4.5	1.3	Pool boiling in saturated helium
HTS SC link cable (P1, P5 & P7)	4.5-17	1.3-1.2	Force flow in helium gas
HTS SC link screen (P1, P5 & P7)	20-100	1.2-1.1	Force flow in helium gas
HTS current lead (P1, P5 & P7)	20 - 300	1.2-1.15	Force flow in helium gas
Q1-Q2-Q3 string (P1 & P5)	1.9	1.3	In static pressurized superfluid helium via two parallel bayonet heat exchanger Φ 77 mm
D1 & Corrector Package (CP) string (P1 & P5)	1.9	1.3	In static pressurized superfluid helium via two parallel bayonet heat exchanger Φ 49 mm
D2 (P1 & P5)	1.9	1.3	In static pressurized superfluid helium via a bayonet heat exchanger Φ 54 mm
Q4 (P1 & P5)	1.9	1.3	In static pressurized superfluid helium via a bayonet heat exchanger Φ 54 mm
Crab-cavity module (P1 & P5)	2.0	0.03	Pool boiling in saturated superfluid helium
Q5 (P1 & P5)	4.5	1.3	Pool boiling in saturated helium
Q6 (P1 & P5)	4.5	1.3	Pool boiling in saturated helium

If this alternative cooling is retained, in order to limit the number of distribution lines, the thermal shields will be cooled with the same temperature range (40-60 K).

4. Cryogenic plant upgrade

4.1. Impact on existing cryogenic plants

Table 2 gives the heat loads at different temperature levels to be extracted by the sector cryogenic plants which have no longer to take care of insertion regions at their extremities and SRF modules. The corresponding reduction of loads allows compensating the load increase on the sector beam screens while increasing the margin on the 1.9 K level. With respect to the installed capacities at different temperature levels and with efficient scrubbing of the beam screen, significant overcapacity factors between 1.3 and 2.2 are still existing and no specific upgrade is required.

Table 2. Heat loads and installed capacity of high-load sector cryogenic plants (low-load sectors in brackets).

Temperature level	Heat loads [kW]	Installed capacity [kW]	Overcapacity factor [-]
50-75 K	20.5 (20.5)	33 (31)	1.6 (1.5)
4.6-20 K with efficient beam scrubbing	5.5 (5.9)	7.7 (7.6)	1.4 (1.3)
4.6-20 K without efficient beam scrubbing	28.5 (28.8)	7.7 (7.6)	0.3 (0.3)
1.9 K	1.1 (0.93)	2.4 (2.1)	2.1 (2.2)
20-290 K (current leads)	33.6 (28.8)	57.5 (37.9)	1.7 (1.3)

4.2. New cryogenic plant for Point 4 insertion

Fig. 3 shows the upgraded cryogenic architecture of the point-4 insertion. A warm compressor station (WCS) is located in a noise-insulated surface building and is connected to a helium buffer storage. A lower cold box (LCB) is located in the UX45 cavern and is connected to a cryogenic distribution valve box (DVB) as well located in the UX45 cavern. Main cryogenic distribution lines connect the cryo-modules to the distribution valve box. Auxiliary cryogenic distribution lines interconnect the new infrastructure with the existing QRL service modules (SM) to allow redundancy cooling by adjacent-sector cryogenic plants.

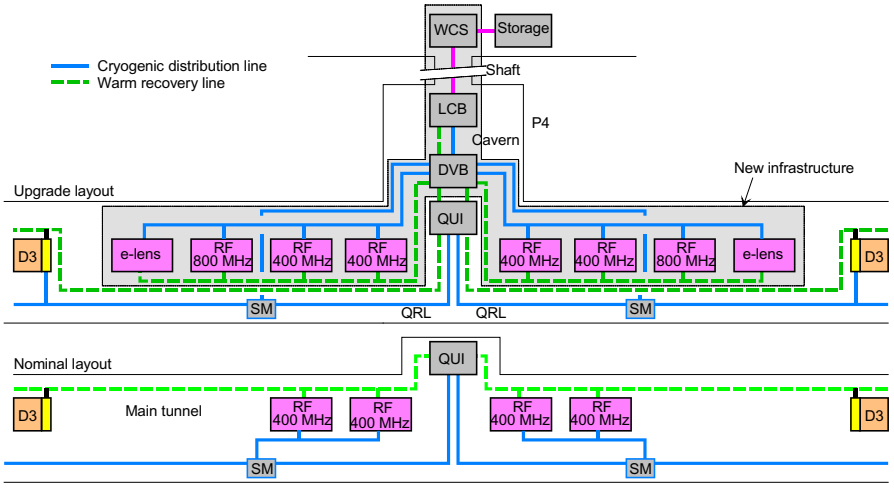

Fig. 3. Nominal and Upgrade cryogenic architecture at Point 4.

Table 3 gives the heat loads and the installed capacity of the point 4 cryogenic plant required at the different temperature levels and calculated with an uncertainty coefficient of 1.5 on the static heat inleaks and with an overcapacity factor 1.5. This cryogenic plant will require an equivalent capacity of about 6 kW at 4.5 K.

Table 3. Heat loads and installed capacity of cryogenic plant at point 4.

Temperature level	Static heat inleaks [W]	Dynamic heat load [W]	Installed capacity [W]	Equivalent installed capacity @ 4.5 K [kW]	
4.5 K	1144	1736	5223	5.6	5.8
50-75 K	1000	0	2250	0.2	

4.3. New cryogenic plants for point 1 and 5 insertions

Fig. 4 shows the upgraded cryogenic architecture of the points 1 and 5 high-luminosity insertions. A warm compressor station (WCS) is located in a noise-insulated surface building and is connected to a helium buffer storage. An upper cold box (UCB) is located in a ground level building and is connected to a cold quench buffer (QV) located at ground level. One or two cold compressor boxes (CCB) are located in underground cavern. Two main cryogenic lines (one per half-insertion) distribute helium to the insertion cryo-assemblies. Finally, two interconnection valve boxes interconnect the new infrastructure with existing QRL cryogenic line to allow partial redundancy with the cryogenic plants of adjacent sectors. Table 4 gives the heat loads and installed capacity of the cryogenic plants at points 1 and 5 required at the different temperature levels and using the same uncertainty (1.5) and overcapacity (1.5) factors than for point 4.

Table 4. Heat loads and installed capacity of cryogenic plant at point 1 and 5.

Temperature level	Static heat inleaks [W]	Dynamic heat load [W]	Installed capacity [W]	Dynamic range [-]	Equivalent installed capacity @ 4.5 K [kW]	
1.9 K	433	1380	3045	7	12	
4.5 K	196	8	452	2	0.5	
4.6-20 K	154	2668	4348	28	2.4	18
50-75 K	4900	0	7350	2	0.5	
20-290 K	22200	22200	83200	4	2.6	

The cryogenic plants will require an equivalent capacity of about 18 kW at 4.5 K, including about 3 kW at 1.8 K which is higher than the 2.4-kW installed capacity of a LHC sector which corresponds to the present state-of-the-art

for the cold compressor size. Consequently, larger cold compressors have to be studied and developed, or parallel cold compressor trains have to be implemented (one 1.5 kW train per half insertion), or, the first stage of cold compression has to be duplicated to keep the machine within the available size. Large dynamic ranges have also to be implemented especially for the cold-mass and beam screen cooling.

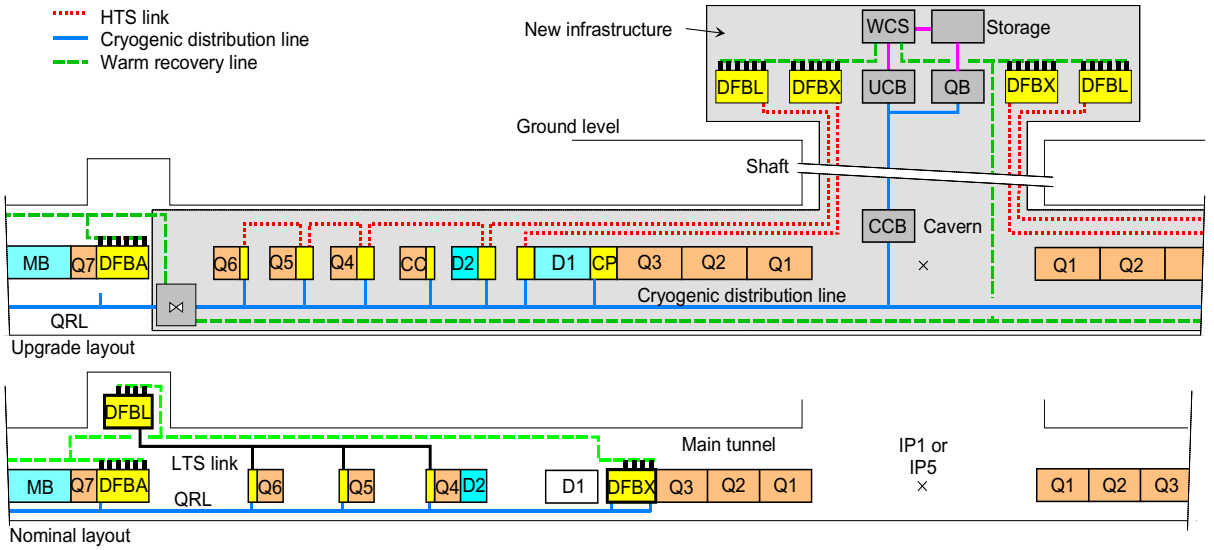

Fig. 4. Nominal and upgraded cryogenic architecture at Points 1 and 5.

5. Conclusion

The HL-LHC project will require a large cryogenic upgrade with new cryogenics challenges. New cooling circuits must be designed to extract up to 13 W/m on 1.9 K cold-mass superconducting cables while keeping sufficient margin with respect to resistive transition limit, as well as up to 23 W/m on inner-triplet beam-screens with possibly a different operating range (40-60 K) and with a large dynamic range which will require specific cryogenic-plant adaptation studies. New cooling method of HTS links, current feed boxes and crab-cavities must be developed and validated. The resistive transition containment and helium recovery via cold buffering must be designed for efficient operation. Concerning cryogenic plants, larger 1.8 K refrigeration capacities beyond the present state-of-the-art must be developed including large capacity (1500/3000 W) sub-cooling heat exchangers. This upgrade will be implemented within to main phases. During the second long shutdown of LHC in 2018-2019 calendar years, the upgrade at point 2, point 7 and point 4 will be implemented. The remaining part will be implemented during the third long shutdown of LHC in 2023-2025 calendar years.

References

Baglin, V., Lebrun, Ph., Tavian, L., van Weelderen, R., 2012, Cryogenic beam screens for high-energy particle accelerators, Proceedings of ICEC24, Fukuoka, Japan: 629-634.

Calaga, R., 2012, Crab cavities for the LHC upgrade, Proceedings of the Chamonix 2012 Workshop on LHC Performance, Chamonix, France.

Granieri, P., Hincapié, L., van Weelderen, R., 2013, Heat transfer through the electrical insulation of Nb3Sn cables, Proceedings of MT23, Boston, USA.

Granieri, P., van Weelderen, R., 2013. Deduction of steady-state cable quench limits for various electrical insulation schemes with application to LHC and HL-LHC Magnets, Proceedings of MT23, Boston, USA.

Rossi, L., and O. Brüning, O., 2012, High Luminosity Large Hadron Collider A description for the European Strategy Preparatory Group, CERN-ATS-2012-236.

Todesco, E., *et al*., 2013, A First Baseline for the magnets in the high-luminosity LHC insertion regions, Proceedings of MT23, Boston, USA.

Todesco, E., *et al.*, 2012. Design studies for the low-beta quadrupoles for the LHC luminosity upgrade, Proceedings of ASC 2012, Portland, Oregon, USA.